Soil Water Evaluation Using a Hydrologic Model and Calibrated Sensor Network

D. C. Hymer,* M. S. Moran, and T. O. Keefer

ABSTRACT

Studies show that it may be possible to combine satellite-derived soil water maps with soil–vegetation–atmosphere transfer (SVAT) models to obtain spatially distributed, temporally continuous information on vadose zone water contents. However, before this method can be instituted, it is essential to determine the ability of a SVAT model to simulate vadose zone soil water contents. A study was designed to evaluate the simultaneous heat and water (SHAW) model by comparing its soil water predictions with measured soil water contents collected by electrical resistance sensors (ERS) during the Monsoon '90 multidisciplinary field experiment. ERS collected hourly soil water measurements at 5-, 15-, and 30-cm depths in a shrub-dominated site [*Larrea tridentada* (Sessé & Moc. ex DC.) Coville] with large bare interspace areas. Data collected by the ERS were calibrated to time domain reflectometer (TDR) sensor measurements placed adjacent to the ERS using an in situ calibration technique. Results indicated that the SHAW model overestimated soil water at each depth by 0.02 m^3 m^{-3} under bare soil and underestimated soil water at each depth under shrub cover by 0.02 m^3 m^{-3}. The ability of the model to simulate ERS water content values gives it the potential to be periodically updated with remotely sensed data to predict vadose zone soil water content over large areas at high temporal resolutions.

Soil water plays a key role in the transfer of energy and mass between land surfaces and the atmosphere, rivers, and aquifers (Blyth et al., 1993). In fact, the spatial and temporal distribution of soil water is a critical part of many disciplines including agriculture, forest ecology, hydroclimatology, civil engineering, water resources, and ecosystem modeling (Houser, 1996). Unfortunately, difficulties with soil water measurement techniques have made long-term regional data sets difficult to compile. Therefore, it is important to define an approach to monitor, characterize, and model soil water over a wide range of temporal and spatial scales (Islam and Engman, 1996).

Long-term soil water data sets are rare because many soil water sampling techniques (e.g., gravimetric, neutron probe, and time domain reflectometry) can be labor intensive and difficult to learn without appropriate training. Gravimetric measurements are simple and accurate, but are destructive and require at least 24 h of post-processing. Traditional time domain reflectometer (TDR) sensors yield accurate measurements with calibration, but are expensive and take spatially discrete measurements. Neutron probes are nondestructive and can sample over great depths, but are expensive and potentially hazardous without appropriate training. Fiberglass electrical resistance sensors (ERS) connected to automated dataloggers, however, can record temporally continuous data with little maintenance over long time periods. Like many soil water sensors, ERS require a calibration to convert a measured signal to volumetric water content. Seyfried (1993) documented two difficulties with calibrating these sensors: (i) They exhibit large variability among individual sensors; and (ii) They are sensitive to variations in soil properties and temperature. This same study, however, demonstrated that a field calibration of ERS to TDR sensors accounted for site-specific soil conditions and yielded reasonable estimates of soil water (± 0.05 m^3 m^{-3}).

Hydrologic models can also be used to estimate soil water at various spatial and temporal resolutions. In particular, soil–vegetation–atmosphere transfer (SVAT) models are gaining attention as a means of better representing interactions between the soil and atmosphere. One of these SVAT schemes, the simultaneous heat and water (SHAW) model, is a detailed physical-process model capable of simulating the effects of a multispecies plant canopy on heat and water transfer at the soil–atmosphere interface (Flerchinger, 1987). Unfortunately, numerous studies have shown that SVAT models in general are subject to errors as a result of simplified model physics and complicated meteorological and site-characteristic inputs (Houser, 1996; Henderson–Sellers, 1996; Desborough et al., 1996; Lau et al., 1996). Consequently, SVAT models do not always produce reliable soil water estimates. Furthermore, these models usually require extensive meteorological and site-characteristic input parameters that can be difficult to acquire.

Because both in situ soil measurements and SVAT models are problematic, no large-scale soil water information exists at the spatial and temporal resolutions required to investigate how soil water can influence various land and atmospheric processes. Recent studies have proposed that images from synthetic aperture radar (SAR) sensors can be used to map spatially distributed soil water patterns within 5 cm of the surface (Engman and Chauhan, 1995; Sano, 1997). This method would provide a way to estimate soil water at large-scale resolutions not achievable with in situ measurements or modeling methods. Unfortunately, many studies require vadose zone soil water measurements rather than surface soil water measured by the SAR sensor. Furthermore, soil water information from orbiting SAR sensors would only be available at the time of the satellite overpass, which could be as infrequent as once a month.

By combining SAR-derived surface soil water maps

D.C. Hymer, NASA–GSFC Hydrologic Sciences Branch, Code 974, Greenbelt, MD 20771; M.S. Moran and T.O. Keefer, USDA–SWRC, 2000 E. Allen Road, Tucson, AZ 85719. Received 5 Aug. 1998. *Corresponding author (dhymer@hydro4.gsfc.nasa.gov).

Published in Soil Sci. Soc. Am. J. 64:319–326 (2000).

Abbreviations: CI, confidence interval; ERS, electrical resistance sensors; MBE, mean bias error; MPD, mean percentage difference; RMSE, root mean square error; SAR, synthetic aperture radar; SHAW, simultaneous heat and water [model]; SVAT, soil–vegetation–atmosphere transfer [model]; TDR, time domain reflectometer; θ_v, volumetric water content.

with a SVAT scheme, it may be possible to obtain spatially distributed, temporally continuous information on vadose zone soil water measurements. That is, using techniques described by Sano (1997) and Moran et al. (1998), SAR images may be converted into surface soil water maps suitable for SVAT processing. Using these data along with required model inputs (meteorological, initialization, and site parameters), one may utilize the SVAT scheme to model soil water at depth, between and during satellite overpasses. At each subsequent satellite overpass, model parameters may be reinitialized according to the newly acquired SAR-derived soil water data, ultimately yielding a large-scale, temporally continuous soil water data set. In theory, this synthesis should result in less error than with remotely sensed data or the SVAT model used alone.

The first step in developing such a combined approach is to investigate the accuracy and precision of a SVAT model to estimate surface and vadose zone soil water over time. In this study, we calibrated a network of in situ ERS to create a long-term, temporally continuous soil water data set that could be used to study the SHAW model. Two objectives of this research were to (i) develop a 12-mo, hourly soil water data set at 5-, 15-, and 30-cm depths under three bare and three shrub-cover surfaces, and (ii) study the relationship between measured and predicted soil water contents.

MATERIALS AND METHODS

Site Description

Soil water data were collected from the Lucky Hills subwatershed in the Walnut Gulch Experimental Watershed located in the vicinity of Tombstone, AZ (Renard et al., 1993). The Lucky Hills subwatershed was instrumented in 1990 by the USDA–ARS as part of the interdisciplinary Monsoon '90 field campaign for continuous measurement of local energy conditions and surface energy balance (Kustas and Goodrich, 1994) (Fig. 1). Standard measurements included soil water, soil temperature, soil heat flux, relative humidity, incoming solar radiation, net radiation, wind speed, and wind direction (Stannard et al., 1994).

The Lucky Hills subwatershed is at a 1371-m elevation and has an average annual precipitation of 300 mm, 70% of which falls during the summer monsoon between July and September (Tiscareno–Lopez, 1991). This 1.46-ha area is dominated by creosote bush (*Larrea tridentada*) at 2- to 5-m spacing (26% cover) with surface rock percentages ranging from 0 to 46% (Kustas and Goodrich, 1994). Larger creosote shrubs are about 1-m tall and can be characterized by a spatially averaged leaf-area index value of 0.4 (Flerchinger et al., 1998). The dominant soil type in the subwatershed is the Lucky Hills series with a very gravelly sandy-loam texture (Table 1). Rock content of the soil profile is 28% by volume between 0 and 5 cm and then decreases with depth.

Sensor Placement and Description

Eighteen pairs of ERS and TDR probes were installed horizontally into trench faces under three bare and three shrub-covered surfaces at 5-, 15-, and 30-cm depths according to procedures outlined by Bach (1991). Detailed descriptions of each trench location and its respective surface vegetation and profile characteristics are also presented. ERS used in this study were similar to those described by Colman and Hendrix (1949) and identical to those of Amer et al. (1994). Each 4- by 4-cm ERS contains several fiberglass layers wrapped around stainless-steel screens that are connected by wire leads to an automated datalogger. Original laboratory- and site-calibration procedures for ERS used in the experiment were described by Amer et al. (1994). Three-pronged TDR probes constructed by the USDA–ARS were placed adjacent to the ERS at each depth in the trenches (Bach, 1991). Dataloggers recorded hourly ERS values and ARS scientists collected TDR samples in the field at time intervals varying from daily to biweekly between August 1990 and July 1991. ERS readings were stored as a series of resistances (Ω) while TDR readings were calibrated to yield the volumetric water content (θ_v) of the soil. ERS readings were averaged, respectively, using data collected from three trenches under bare soil and three trenches under creosote cover. In this study, it was assumed that TDR measurements represent the actual water content of the soil.

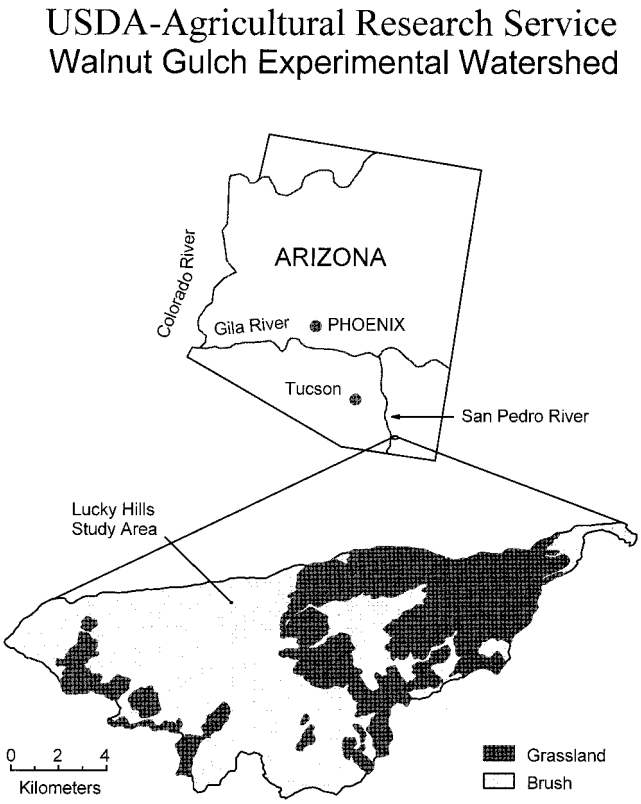

Fig. 1. Map of the Walnut Gulch Experimental Watershed showing its geographical location in the state of Arizona.

Calibration

Seyfried (1993) found a nonlinear relationship between TDR-measured θ_v and ERS resistance values, as did Amer et al. (1994). Based on these analyses, a modified nonlinear calibration equation (Eq. [1]) was developed with the form

$$Y = aX^b \quad [1]$$

where Y is TDR measured θ_v, a and b are parameters to be optimized, and X is ERS-measured resistance (Ω). This expression (Eq. [1]) was modified from the original calibration expression used by Amer et al. (1994) by eliminating an additive coefficient so that each parameter, when optimized, was significantly different from zero. This transformation was de-

Table 1. Description of physical characteristics of the Lucky Hills soil unit.†

Parameter	Lucky Hills unit
Soil classification	Coarse-loamy, mixed, thermic Ustochreptic Calciorthid
Slope	0–15%
Landform	Fan terraces
Particle size class	Very gravelly sandy loam
Drainage class	Well drained

† Breckenfeld (1995) and Bach (1991).

signed so that the model would be more sensitive to water content changes at lower resistance values. Individual in situ field calibrations were completed for all 18 ERS–TDR pairs by optimizing *a* and *b* parameters using nonlinear curve fitting techniques with a statistical software package. TDR and ERS measurements collected at identical times between August 1990 and July 1991 were used in each calibration. The average sample size used in each calibration was 78, but ranged from 46 to 103, due to instrumentation problems and measurement errors. Statistical tests were used to show that the *a* and *b* parameter values were significantly different from zero ($\alpha = 0.05$ and $\alpha = 0.10$).

In this analysis, it was assumed that the variability in θ_v measurements could be attributed to the calibration errors of the TDR and ERS. Bach (1991) described the installation and calibration procedures of the TDR probes used in this experiment. These calibrations did not account for temperature fluctuations that could affect TDR readings. Halbertsma et al. (1994) found that TDR readings are only slightly influenced by changing temperature and salinity conditions; and Dalton (1992) found that TDR readings are independent of temperature in soil textures finer than sand. Without considering these limitations, calibrations revealed that for the 95% confidence interval (95% CI), the root mean square error (RMSE) of the TDR measurements was 0.02 $m^3\ m^{-3}$. Ultimately, the total error in each calibration was quantitatively defined as the square root of the sum of squares for the TDR and ERS RMSE values (Eq. [2]). Quantile plots indicate that residuals for the TDR and ERS showed no serious departure from normality.

$$\text{Total calibration error} = (\text{TDR RMSE}^2 + \text{ERS RMSE}^2)^{1/2} \quad [2]$$

THEORY

The Simultaneous Heat and Water Model

The SHAW model is a detailed process model that simulates heat and water movement through a plant residue–soil system (Flerchinger, 1987). A vertical, one-dimensional profile extending from the vegetation canopy to a specified depth within the soil is represented by this model. At various points in this vertical profile, user-defined nodes represent various canopy and soil layers. For each of these nodes, interrelated water, water vapor, heat, and solute fluxes are calculated.

Daily or hourly weather conditions above the upper boundary and soil conditions at the lower boundary define heat and water fluxes into the system (Flerchinger, 1987). Specifically, air temperature, wind speed, relative humidity, and solar radiation define upper-boundary conditions while temperature and water contents at the bottom of the soil profile define lower-boundary conditions. Other inputs required by the model include general site parameters, textural and physical properties of the soil, and initial temperature and water-content values. Model outputs include a summary of water balance, in addition to temperature, water, and solute profiles.

Table 2. Original† and revised‡ soil textural and hydrologic parameters at the Lucky Hills soil unit.

Simulation	Bulk density	Saturated θ_v	Sand	Silt	Clay
	$kg\ m^{-3}$	$m^3\ m^{-3}$	%		
Original	1253	0.53	68.8	19.7	11.4
Revised	1640	0.38	66.0	24.0	10.0

† Flerchinger (1998).
‡ Kustas and Goodrich (1994).

The SHAW model uses a modified form of Richards equation to calculate θ_v at each node, based on water-content values defined at the lower boundary (Flerchinger, 1987). At any frequency, user-defined θ_v values may be used to update lower boundary conditions to improve simulation accuracy. In each case, linear interpolation is used to predict θ_v values between lower boundary θ_v intermediate values.

Model Testing

Two separate trials were used to simulate hourly θ_v under bare and shrub surface cover at 5-, 15-, and 30-cm depths. In both cases, many site parameters were used that were identical to those used in previous simulations completed by Flerchinger et al. (1998). Specific textural and hydraulic soil parameters, however, were modified to match trench data measured directly at the location of the soil water sensors under bare soil and shrub cover (Table 2). Surface and root plant parameters were used in shrub-cover simulations only and were defined by Flerchinger et al. (1998). Bare-soil simulations did not include root-distribution parameters because no discrete measurements could be included. Hourly meteorological data inputs were collected from meteorological-energy flux (METFLUX) towers located in the subwatershed (Kustas and Goodrich, 1994). Initial and final soil temperature readings for the simulation period were recorded by thermocouples installed adjacent to ERS and TDR probes in the soil at 5-, 15-, and 30-cm depths. Because soil temperature values have only a minor effect on modeled soil water content values, intermediate temperature values were not used in these simulations. Finally, θ_v values taken by TDR probes at the same depths were used as initial and intermediate model inputs. Specifically, 13 intermediate lower-boundary (30 cm) θ_v values at approximately 30-d intervals were used to update model simulations.

Regression analysis was used as a tool to evaluate the ability of the SHAW model to simulate the respective averages of calibrated, hourly ERS θ_v values at 5-, 15-, and 30-cm depths under bare soil and shrub cover. Furthermore, statistical discrepancies between measured and simulated hourly θ_v values were evaluated by calculating the mean bias error (MBE), mean percentage difference (MPD) and RMSE. Definitions for each are given in Table 3. Finally, hourly measured and

Table 3. Description and definition of model performance measures.†

Measure	Description	Mathematical definition
MBE	Mean bias error of model predictions compared to observed values.	$\frac{1}{n}\sum_{i=1}^{N}(\hat{Y}i - Yi)$
RMSE	Root mean square error measures how widely model predictions are dispersed from the average value.	$\sqrt{\frac{n\sum y^2 - (\sum y)^2}{n(n-1)}}$
MPD	Mean percentage difference indicates the deviation of modeled predictions from observed values as a percentage.	$\left[\left(\frac{1}{n}\sum_{i=1}^{n}\left\|\hat{Y}_i - Y_i\right\|\right)\Big/\hat{Y}\right]\cdot 100$

† Y = simulated values, $\bar{Y}$ = mean of observed values, n = sample size.

Table 4. Optimized parameter (*a* and *b*) and coefficient of determination (R^2) values for individual electrical resistance sensors.

Sensor trench–depth (cm)	*a*	*t* statistic† *a* parameter	*b*	*t* statistic† *b* parameter	R^2
1–5	15.62	19.39	−0.45	−9.37	0.58
1–15	27.88	16.70	−0.17	−10.87	0.66
1–30	27.59	21.36	−0.11	−11.37	0.61
2–5	26.32	11.36	−0.21	−9.80	0.65
2–15	19.88	28.79	−0.19	−16.80	0.80
2–30	15.67	38.62	−0.14	−19.90	0.81
3–5	29.43	12.94	−0.21	−11.37	0.72
3–15	23.63	31.91	−0.13	−17.71	0.84
3–30	20.35	12.24	−0.11	−5.57	0.33
4–5	18.99	19.80	−0.40	−11.39	0.71
4–15	22.15	21.69	−0.21	−13.53	0.82
4–30	15.27	22.50	−0.65	−9.33	0.58
5–5	17.87	37.09	−0.10	−12.56	0.74
5–15	16.97	47.09	−0.27	−12.39	0.70
5–30	15.07	35.95	−0.08	−11.26	0.62
6–5	27.89	12.43	−0.24	−11.19	0.67
6–15	25.34	19.52	−0.18	−13.03	0.73
6–30	25.34	39.17	−0.15	−23.39	0.88

† *t* tests at $\alpha = 0.05$ and $\alpha = 0.10$.

simulated θ_v values were plotted as a time series to analyze how well the SHAW model could simulate water profile dynamics.

RESULTS AND DISCUSSION

Calibration Statistics

Optimized parameter (Eq.[1]) and coefficient of determination (R^2) values for all 18 ERS–TDR probes are given in Table 4. In all cases, *t* tests ($\alpha = 0.05$ and $\alpha = 0.10$) indicated that optimized *a* and *b* parameters were significantly different from zero, demonstrating that the calibration function effectively translated resistance values into θ_v without yielding an average water content. Data presented in Fig. 2 show a calibration curve with matched TDR and ERS values ($R^2 = 0.88$). Clearly, resistance values approach zero as θ_v increases. In some cases, the calibration functions showed considerable scatter, especially at higher resistance values (>1000 Ω). Each calibration function, however, accounted for this scatter at high resistances by yielding a constant θ_v value above 1000 Ω.

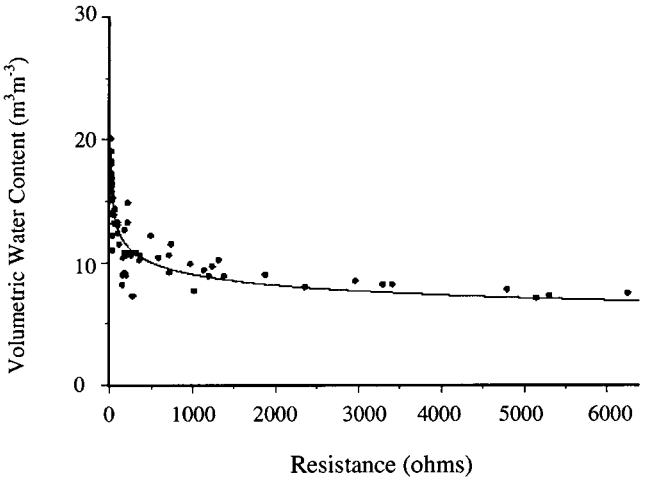

Fig. 2. Calibration curve for electrical resistance sensors ($R^2 = 0.88$). Points represent matched time domain reflectometer and electrical resistance sensor measurements used to derive the calibration curve represented by the solid line.

Table 5. Estimated calibration error for individual electrical resistance sensors (ERS).

Sensor trench–depth (cm)	Calibration error
	%
1–5	3.0
1–15	3.6
1–30	3.4
2–5	3.0
2–15	2.8
2–30	2.4
3–5	2.6
3–15	2.4
3–30	3.9
4–5	2.9
4–15	2.3
4–30	3.6
5–5	2.3
5–15	2.5
5–30	2.6
6–5	3.0
6–15	2.6
6–30	2.4
Avg. (18 sensors)	2.9

† Equation 2: calibration error = time domain reflectometry $RMSE^2$ + ERS $RMSE^2)^{1/2}$.

Coefficient of determination (R^2) values for individual sensor calibrations at all three depths ranged from 0.33 to 0.88 (mean $R^2 = 0.69$) (Table 4). Wide ranges of R^2 values at each depth and in various trenches indicate that calibration variability was the result of individual sensors and not soil differences. These findings are consistent with the calibration results reported by Seyfried (1993). Calibration parameters were applied to each of the 18 individual ERS. In all cases, estimated θ_v values below the calculated residual water content of the soil were adjusted to a threshold value of 3.4% (Woolhiser et al., 1990).

Calibration Error

Individual sensor calibration errors were estimated as the square root of the sum of the squares for the TDR and ERS RMSE values (95% CI) (Table 5) (Eq. [2]). The total average calibration error for all 18 sensors was ± 0.029 m^3 m^{-3} and ranged between 0.023 and 0.039 m^3 m^{-3} for individual sensors. These findings are similar to those of Seyfried (1993), who found an average error of 0.05 m^3 m^{-3} in a similar calibration experiment.

Model Evaluation: Bare Soil

Data presented in Table 6 summarize the results of statistical analyses used to evaluate the performance of

Table 6. Calculated mean bias error (MBE), mean percentage difference (MPD), root mean square error (RMSE), and coefficient of determination (R^2) statistics for electrical resistance sensors and Simultaneous Heat and Water model water content values under bare soil and shrub cover.

Location	MBE	MPD	RMSE	R^2
	m^3 m^{-3}	%	m^3 m^{-3}	
Bare 5 cm	+0.04	39.13	0.02	0.77
Bare 15 cm	+0.02	15.93	0.01	0.77
Bare 30 cm	+0.01	8.83	0.01	0.82
Shrub 5 cm	−0.01	23.61	0.02	0.79
Shrub 15 cm	−0.02	26.30	0.01	0.89
Shrub 30 cm	+0.01	4.52	0.01	0.92

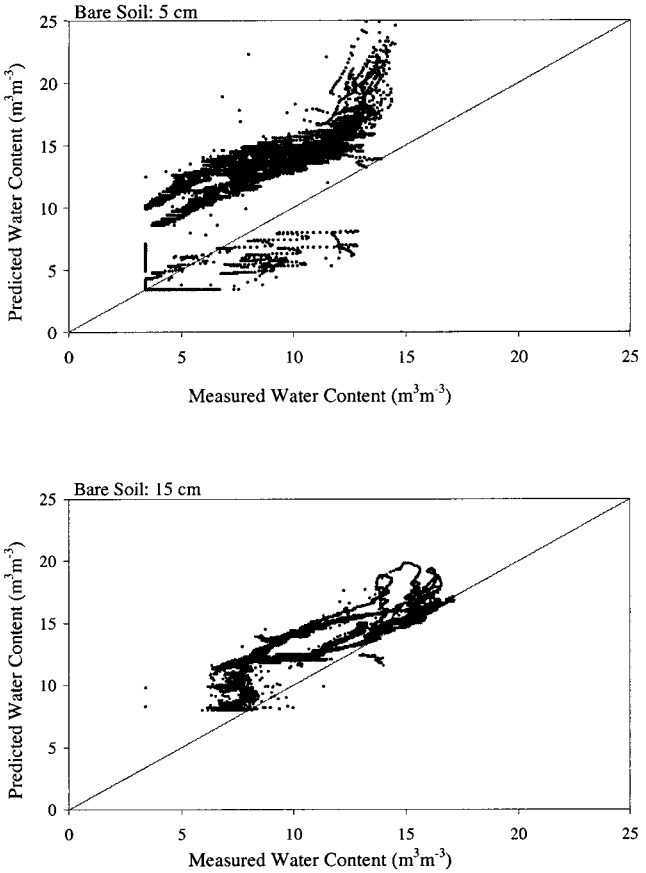

Fig. 3. Scatterplot of predicted Simultaneous Heat and Water model volumetric water content values vs. calibrated electrical resistance sensor volumetric water content measurements at 5- and 15-cm depths under bare soil.

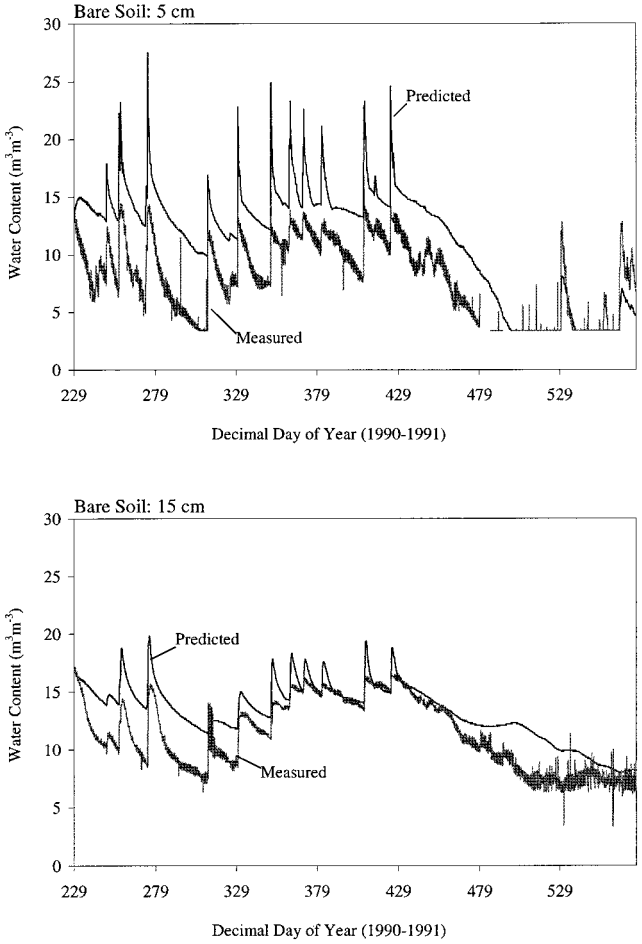

Fig. 4. Predicted Simultaneous Heat and Water model volumetric water content values and calibrated electrical resistance sensor volumetric water content measurements at 5- and 15-cm depths under bare soil plotted as an hourly time series (August 1990–July 1991).

the SHAW model under bare soil. In this case, the MBE between measured and simulated θ_v gradually decreased from 0.04 m^3 m^{-3} at a 5-cm depth to 0.01 m^3 m^{-3} at a 30-cm depth. This trend, however, was expected because it was consistent with the SHAW model structure. That is, the SHAW model calculates surface and intermediate θ_v values based on lower-boundary measurements updated in the simulation. MPD and RMSE values reflected this same trend, indicating that the model did not simulate θ_v well at shallower depths.

The scatterplot of measured and simulated θ_v values at 5 cm under bare soil produced a bimodal distribution (Fig. 3). The bimodal distribution in this plot can be characterized by temporal association. That is, the lower group of matched points falls below the 1:1 line because it shows a period in the driest part of the summer season where the SHAW model is underestimating θ_v. Conversely, the highest cluster on the scatterplot indicates that the model consistently overestimates θ_v in moist conditions. This trend is evident when the data are plotted on a time series (Fig. 4).

Statistical analysis indicates that model simulations improved at 15 cm. MBE, MPD and RMSE values were approximately half as large as those at the 5-cm depth. The scatterplot (Fig. 3) and time series (Fig. 4) of the calibrated ERS and SHAW θ_v values at 15 cm under bare soil reveal that the SHAW model overestimates θ_v throughout the entire simulation period.

At the lower-boundary layer (30 cm), the SHAW model simulated θ_v values well. However, θ_v values at the lower boundary were calculated by using linear interpolation between intermediate θ_v values used as model inputs, and therefore, are expected to be nearly identical to measured θ_v values.

Model Evaluation: Shrub Cover

The results of statistical analyses used to evaluate the performance of the SHAW model under shrub cover are summarized in Table 6. At each depth, SHAW model θ_v values underestimated calibrated ERS θ_v values. MBE, MPD, and RMSE values were lower, on average, than those calculated in the bare-soil simulations but were distributed differently. In this case, MBE and MPD values at the 15-cm depth were higher than those at 5 cm. Similar to the results for bare-soil simulations, MBE and MPD values were lowest at the lower-boundary layer. A possible explanation for the differences between measured and simulated θ_v at 5 and 15 cm may be related to root distribution parameters defined as

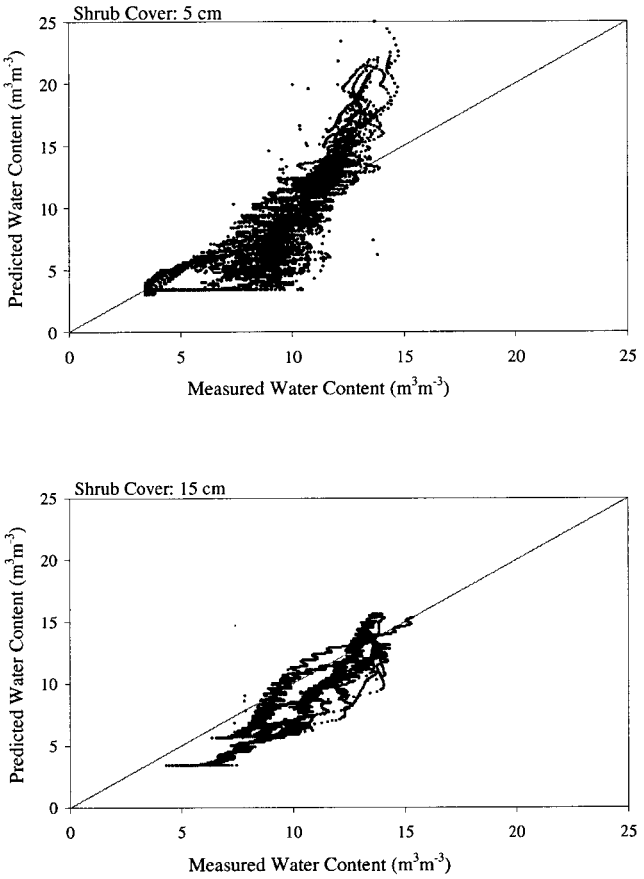

Fig. 5. Scatterplot of predicted Simultaneous Heat and Water model volumetric water content values vs. calibrated electrical resistance sensor volumetric water content measurements at 5- and 15-cm depths under creosote cover.

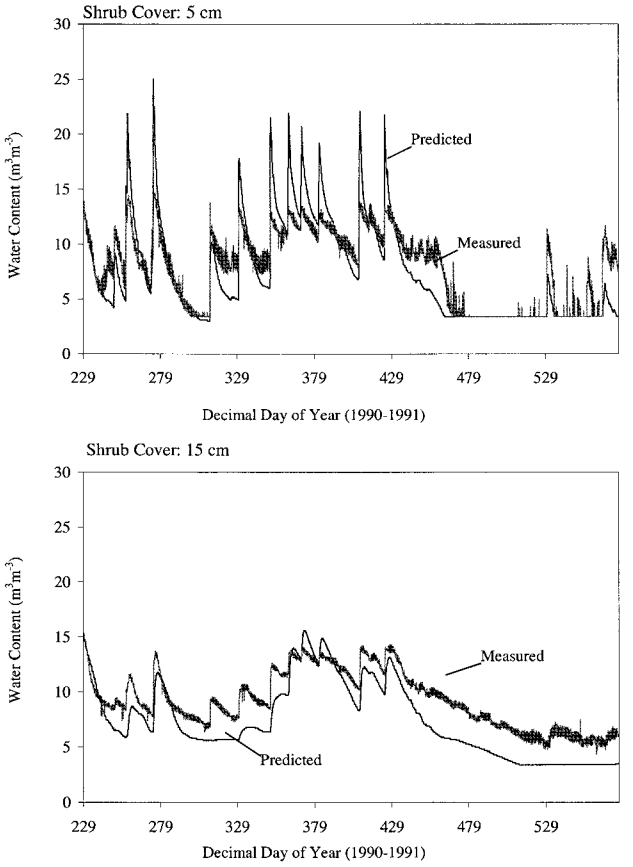

Fig. 6. Predicted Simultaneous Heat and Water model volumetric water content values and calibrated electrical resistance sensor volumetric water content measurements at 5- and 15-cm depths under creosote cover plotted as an hourly time series (August 1990–July 1991).

model inputs. That is, root extraction of soil water at both depths may have been too high, ultimately causing the model to underestimate θ_v. A second possible explanation for the discrepancy between simulated and measured θ_v may be due to a positive bias in transpiration demand (Jones, 1983). Model estimates of transpiration may have been too high, causing the model profile to lose water, ultimately yielding low θ_v values.

Data presented in Fig. 5 show the scatterplot between measured and simulated θ_v values at 5 cm under shrub cover. In this case, at higher values, the SHAW model overestimated θ_v, while at lower values, the SHAW model underestimated θ_v. When these data are plotted as a time series, the high peaks in this graph show where SHAW overestimated θ_v, while the driest periods (DDOY 440–530) indicate where SHAW underestimated θ_v (Fig. 6).

The scatterplot and time series of measured and simulated θ_v values at the 15-cm depth under shrub cover are presented in Fig. 5 and 6, respectively. These data indicate that during inter-storm periods throughout the year, SHAW θ_v estimates were substantially lower than measured θ_v values. Once again, inaccurate root distribution, a positive bias in transpiration demand, and soil hydraulic properties may be responsible for these discrepant results.

At the lower-boundary layer (30 cm), the SHAW model simulated θ_v values well. However, just as in the bare-soil simulations, θ_v values at the lower boundary are calculated by using linear interpolation between intermediate θ_v values used as model inputs and are expected to be nearly identical.

Model Uncertainty

Simulations under bare soil and shrub cover both indicate that parameter calibrations would improve model estimations of θ_v. Therefore, a sensitivity analysis was performed to examine the response of simulated θ_v with respect to 10% parameter adjustments. That is, by varying individual parameters while holding all others constant, the sensitivity of the SHAW model to individual parameters was determined. In particular, bulk density, saturated hydraulic conductivity, surface roughness, saturated water content, root distribution percentages, and porosity were analyzed. Data presented in Tables 7 and 8 show the change in θ_v for the entire simulation, based upon parameter adjustments under bare soil and shrub cover, respectively.

In both simulations, distinct *peaks* that overestimated measured θ_v were apparent immediately after rainstorm events (Fig. 4 and 6). These peaks suggest that parame-

Table 7. Model parameter sensitivity analysis for simulations completed under bare soil. Δ Input is the change in the input value expressed as a percentage of the actual value. The Change from actual value = | new value − original value |.

Input variable (depth)	Input value	Δ Input	Change from actual value
			$m^3\ m^{-3}$
Bulk density (5 cm)	1640 kg m^{-3}	+10%	0.003
		−10%	0.002
Bulk density (15 cm)	1640 kg m^{-3}	+10%	0.006
		−10%	0.001
Saturated hydraulic conductivity (5 cm)	3.8 cm hr^{-1}	+10%	0.001
		−10%	0.001
Saturated hydraulic conductivity (15 cm)	3.8 cm hr^{-1}	+10%	0.001
		−10%	0.001
Roughness (surface)	0.12 cm	+10%	NC†
		−10%	NC
Saturated water content (5 cm)	0.38 $m^3\ m^{-3}$	+10%	NC
		−10%	0.003
Saturated water content (15 cm)	0.38 $m^3\ m^{-3}$	+10%	NC
		−10%	0.005
Porosity index value (5 cm)	4.35	+10%	0.003
		−10%	0.003
Porosity index value (15 cm)	4.35	+10%	0.003
		−10%	0.002

† NC, no change.

ters identifying soil porosity, saturated conductivity, or saturated water content may have been too high. In each case, with sufficiently large precipitation, the model will saturate the soil layers to the saturated surface porosity, ultimately yielding peaks that overestimate θ_v. Sensitivity analyses indicated that a 10% increase in the porosity index value could change θ_v for the simulation by as much as 0.005 $m^3\ m^{-3}$ (Table 8).

Shrub-cover simulations underestimated θ_v values at 5- and 15-cm depths during inter-storm periods. A possible source of these discrepancies may be attributed to root-distribution parameters rather than the soil-hydraulic properties highlighted in Tables 7 and 8. If the root-distribution values were too high, water extraction by the plant roots would be too large, ultimately producing unrealistically low θ_v values. Sensitivity analyses indicate, however, that a 10% adjustment will change θ_v by only 0.001 $m^3\ m^{-3}$. Therefore, only major adjustments to root-distribution parameters will significantly affect modeled θ_v.

As one may surmise, changing a combination of hydraulic and physical parameters, rather than a single parameter, would be the best way to calibrate the SHAW model. It is clear from these analyses that peaks and drying rates would be influenced by a combination of many hydrologic parameters including porosity, saturated hydraulic conductivity, root distribution, and bulk density.

DISCUSSION

In future studies, it will be critical to examine the physical structure of the SHAW model to determine if it could be linked with remotely sensed data. That is, one must determine if the model could be modified to use remotely sensed soil water values to update and

Table 8. Model parameter sensitivity analysis for simulations completed under shrub cover. Δ Input is the change in the input value expressed as a percentage of the actual value. The Change from actual value = | new value − original value |.

Input variable (depth)	Input value	Δ Input	Change from actual value
			$m^3\ m^{-3}$
Bulk density (5 cm)	1640 kg m^{-3}	+10%	0.002
		−10%	0.002
Bulk density (15 cm)	1640 kg m^{-3}	+10%	0.003
		−10%	0.001
Saturated hydraulic conductivity (5 cm)	3.8 cm hr^{-1}	+10%	NC
		−10%	0.001
Saturated hydraulic conductivity (15 cm)	3.8 cm hr^{-1}	+10%	0.001
		−10%	0.001
Roughness (surface)	0.12 cm	+10%	NC†
		−10%	NC
Saturated water content (5 cm)	0.38 $m^3\ m^{-3}$	+10%	NC
		−10%	NC
Saturated water content (15 cm)	0.38 $m^3\ m^{-3}$	+10%	NC
		−10%	0.001
Porosity index value (5 cm)	4.35	+10%	0.005
		−10%	0.004
Porosity index value (15 cm)	4.35	+10%	0.005
		−10%	0.004
Root distribution percentage	20%	+10%	0.001
		−10%	0.001

† NC, no change.

predict θ_v at various depths. Currently, the model structure is designed so that θ_v values calculated at nodes in the user-defined soil profile are directly influenced by water content changes at the lower boundary. Therefore, major modifications must be completed so that the SHAW model will calculate the soil water profile based on θ_v values defined at the surface by remotely sensed inputs.

CONCLUSIONS

The dual objectives of this study were to produce a complete, 12-mo soil water data set at three depths, and to use these data to investigate the accuracy and precision of SHAW model surface and vadose zone soil water estimates.

Individual, in situ calibrations of ERS resistance values with TDR θ_v measurements worked well. An hourly soil water data set for a 12-mo period was composed for six replicate sites at three different depths. This simple calibration procedure demonstrated the utility of the ERS for use in future soil water studies. That is, high-frequency ERS measurements, although inaccurate, were easily calibrated with accurate, low-frequency TDR measurements to yield a large, temporally continuous θ_v data set.

In general, the SHAW model simulated annual and diurnal θ_v patterns well (Fig. 4 and 6). However, under bare soil, θ_v values were consistently overestimated while under shrub cover, θ_v values were consistently underestimated. These simulation errors may be attributed to errors in model dynamics, model parameters, or error in sensor calibration. In any case, model calibration and modification will be required so that remotely sensed θ_v values may be assimilated as primary inputs.

With appropriate modifications, the SHAW model may be used to model soil water at depth, between and during satellite overpasses. Ideally, SHAW-model parameters could be initialized by SAR-derived surface soil water estimates to yield a large-scale, temporally continuous soil water data set. Ultimately, this synthesis would provide an effective way to monitor, characterize, and model soil water over a wide range of temporal and spatial scales.

ACKNOWLEDGMENTS

The authors acknowledge Gerald Flerchinger, Dave Toll, Paul Houser, Mike Jasinski, Leslie Bach, Saud Amer, Bill Kustas, Gary Richardson, Jim Toth, Soroosh Sorooshian, Chawn Harlow, Jim Shuttleworth, Dave Goodrich, staff at the Water Conservation Laboratory (Phoenix, AZ), and the Tombstone field office staff for their efforts. In particular, Ted Engman, Carl Unkrich, Ginger Paige, and Scott Miller deserve thanks for their guidance and support. The authors appreciate the comments and suggestions of the anonymous reviewers. This research was funded, in part, by NASA EOS (NASA NAGW–2425), the Landsat Science Team (NASA S–41396–F), and the Monsoon ’90 project (IDP–88–086).

REFERENCES

Amer, S.A., T.O. Keefer, M.A. Weltz, D.C. Goodrich, and L.B. Bach. 1994. Soil moisture sensors for continuous monitoring. Water Resour. Bull. 30:69–83.

Bach, L. 1991. Time domain reflectometry (TDR) for field water content measurements. USDA–Agricultural Research Service Internal Memo. Southwest Watershed Res. Ctr., Tucson.

Blyth, E.M., A.J. Dolman, and N. Wood. 1993. Effective resistance to sensible and latent heat flux in heterogeneous terrain. Q.J.R. Meteorol. Soc. 19:423–442.

Breckenfeld, D.J., W.A. Svetlik, and C.E. McGuire. 1995. Soil survey of Walnut Gulch Experimental Watershed, Arizona. USDA-SCS, Tucson.

Colman, E.A., and T.M. Hendrix. 1949. The fiberglass electrical soil-moisture instrument. Soil Sci. 67:425–438.

Dalton, F.N. 1992. Development of time-domain-reflectometry for measuring soil water content and bulk soil electrical conductivity. p. 153–159. *In* G.C. Topp et al. (ed.) Advances in measurements of soil physical properties: Bringing theory into practice. SSSA Spec. Publ. 30. SSSA, Madison, WI.

Desborough, C.E., A.J. Pitman, and P. Irannejad. 1996. Analysis of the relationship between bare soil evaporation and soil moisture simulated by 13 land surface schemes for a simple non-vegetated site. J. Global Planetary Change 13:47–56.

Engman, E.T., and N. Chauhan. 1995. Status of microwave soil moisture measurements with remote sensing. Remote Sens. Environ. 51:189–198.

Flerchinger, G.N. 1987. Simultaneous heat and water model of a snow-residue-soil system. Ph.D. diss. Washington State Univ., Pullman.

Flerchinger, G.N., W.P. Kustas, and M.A. Weltz. 1998. Simulating surface energy fluxes and radiometric surface temperatures for two arid vegetation communities using the SHAW model. J. Appl. Meteorol. 37:449–460.

Halbertsma, J., E.V. den Elsen, H. Bohl, and W. Skierucha. 1994. Temperature effects on TDR determined soil water content. p. 35–37. *In* L.W. Petersen and O.H. Jacobsen (ed.) Proc. symp.: Time domain reflectometry applications in soil science, Res. Cent. Foulum, Tjele, Denmark. 16 Sept. 1994. Danish Inst. of Plant and Soil Sci., Lyngby, Denmark.

Henderson-Sellers, A. 1996. Soil moisture simulation: Achievements of the RICE and PILPS intercomparison workshop and future directions. J. Global Planetary Change 13:99–115.

Houser, P.R. 1996. Remote sensing of soil moisture using four dimensional data assimilation. Ph.D. diss. Univ. of Arizona, Tucson.

Islam, S., and T. Engman. 1996. Why bother for 0.0001% of Earth’s water? Challenges for soil moisture research. p. 420. Earth Observ. Syst. Newsp. 22 Sept. 1996.

Jones, H.G. 1983. Plants and microclimate. Cambridge Univ. Press, New York.

Kustas, W.P., and D.C. Goodrich. 1994. Monsoon ’90 preface. Water Resour. Res. 30:1211–1225.

Lau, K.M., J.H. Kim, and Y. Sud. 1996. Intercomparison of hydrologic processes in AMIP GCMs. Bull. Am. Meteorol. Soc. 77:2209–2227.

Moran, M.S., D.C. Hymer, J. Qi, R.C. Marsett, M.K. Helfert, and E.E. Sano. 1998. Soil moisture evaluation using synthetic aperture radar (SAR) and optical remote sensing in semiarid rangeland. p. 199–203. *In* Special Symp. on Hydrol., Am. Meteorol. Soc. Meetings, Phoenix, AZ. 11–16 Jan. 1998. Am. Meteorol. Soc., Boston.

Renard, K.G., L.J. Lane, J.R. Simanton, W.E. Emmerich, J.J. Stone, M.A. Weltz, D.C. Goodrich, and D.S. Yakowitz. 1993. Agricultural impacts in an arid environment: Walnut Gulch case study. Hydrol. Sci. Technol. 9:145–190.

Sano, E.E. 1997. Sensitivity analysis of c- and ku-band synthetic aperture radar data to soil moisture content in a semiarid region. Ph.D. diss. Univ. of Arizona, Tucson.

Seyfried, M.S. 1993. Field calibration and monitoring of soil-water content with fiberglass electrical resistance sensors. Soil Sci. Soc. Am. J. 57:1432–1436.

Stannard, D.I., J.H. Blanford, W.P. Kustas, W.D. Nichols, S.A. Amer, T.J. Schmugge, and M.A. Weltz. 1994. Interpretation of surface flux measurements in heterogeneous terrain during Monsoon ’90. Water Resour. Res. 29:1185–1194.

Tiscareno-Lopez, M. 1991. Sensitivity analysis of the Wepp watershed model. Ph.D. diss. Univ. of Arizona, Tucson.

Woolhiser, D.A., R.E. Smith, and D.C. Goodrich. 1990. KINEROS, a kinematic runoff and erosion model: Documentation and users manual. USDA-ARS rep. ARS-77. U.S. Gov. Print. Office, Washington, DC.